PAPER

A porous PDMS pulsewave sensor with haircell structures for water vapor transmission rate and signal-to-noise ratio enhancement†

Minho Seok,[a] Sunghyun Yoon,[b] Mookyum Kim[a] and Young-Ho Cho [ID] *[a]

We present a porous polydimethylsiloxane (PDMS) pulsewave sensor with haircell structures that improves both water vapor transmission rate (WVTR) and signal-to-noise ratio (SNR). The conventional planar PDMS pulsewave sensors have the problems of low WVTR and low SNR for real-time and long-term pulsewave monitoring. In order to improve WVTR, we fabricated a porous PDMS layer with the thickness of 40 μm and high porosity of 45% by crystallizing and dissolving citric acid powders in PDMS. On the porous PDMS layer, we form haircell structures to increase the skin contact area, thus enhancing SNR. The porous PDMS pulsewave sensor with haircell structures achieved an enhanced WVTR of 486.17 g^{-1} d^{-1} m^{-2} and an SNR of 22.89, respectively, 72% and 757% higher than those of the conventional PDMS pulsewave sensors without haircell structures. Furthermore, the enhanced WVTR is 13% higher than the human skin sweat rate of 432 g^{-1} d^{-1} m^{-2}. The present pulsewave sensor shows strong potential for applications in real-time and long-term pulsewave monitoring with the lower skin irritation and the enhanced SNR.

Introduction

Recently, skin attachable sensors[1–19] for measuring human radial artery pulse have gained significant interest due to their increasing demand for cardiovascular disease detection,[9–11] physical activity monitoring,[12–14] mental stress level evaluation,[15] *etc.* Polydimethylsiloxane (PDMS) is widely used for the skin attachable pulsewave sensors because of its high flexibility, non-toxicity, non-flammability, and biocompatibility. However, conventional PDMS pulsewave sensors have two critical problems: (i) low water vapor transmission rate (WVTR) in the level of 382 g^{-1} d^{-1} m^{-2}, less than the skin sweat rate[20] of 432 g^{-1} d^{-1} m^{-2}, which induces side effects such as skin rash and itchiness[21] for long-term skin attachment; (ii) the low signal-to-noise ratio (SNR) in the level of 2.67 caused by the insufficient contact between planar PDMS and non-flat skin with fine topology. Therefore, for radial artery pulse measurement in daily life, the WVTR and SNR of the conventional PDMS pulsewave sensors needs to be improved.

Typical attempts for WVTR enhancement have been made to increase the porosity of PDMS using three different pore

forming materials: citric acid powders,[22] ethanol and deionized (DI) water,[23] and polystyrene beads.[24] Previous porous PDMS fabrication methods, however, have problems for use in skin-attachable sensors: (1) the porous PDMS[22] layer using the citric acid powders are useful only for thick-film applications (≥10 000 μm) since the large citric acid powders (70–400 μm) extensively bounced off from the substrate at the faster spin (>1000 RPM) required for the thinner layer (Fig. S1†). Consequently, the porous PDMS layer using citric acid powders have a low WVTR in the level of 129 g^{-1} d^{-1} m^{-2}; (2) the porous PDMS layer[23] using ethanol and DI water result in thinner thickness (≥400 μm) with the higher WVTR of 495 g^{-1} m^{-2}, but having the maximum porosity limitation (≤40%); (3) the porous PDMS layer[24] using the polystyrene beads achieve a high WVTR of 530 g^{-1} d^{-1} m^{-2} with a thin thickness (≥250 μm) and a high porosity (≥40%). However, the cost of the polystyrene beads is still expensive (300$/20 g).

In this study, we propose a novel porous PDMS layer for high WVTR, where the pores are formed by the crystallization and dissolution of citric acid in PDMS. The porous PDMS layer, having a thin thickness of 40 μm and a high porosity of 45%, achieve a high WVTR of 596 g^{-1} d^{-1} m^{-2}, which is a 38% higher than the human skin sweat rate. Moreover, the cost of citric acid (3$/20 g) is much cheaper (1% of cost) than polystyrene beads.

A typical study for SNR improvement includes the methods to increase the skin contact area using additional surface structures, such as surface grooves,[25] on flat layers. Compared to the flat surface, the grooved surface increases the skin contact

[a]Department of Bio and Brain Engineering, Korea Advanced Institute of Science and Technology (KAIST), 291 Daehak-ro, Yuseong-gu, Daejeon 34141, Republic of Korea. E-mail: nanosys@kaist.ac.kr

[b]Department of R&D, SK Hynix, 2091, Gyeongchung-daero, Bubal-eup, Icheon-si, Gyeonggi-do 17336, Republic of Korea

† Electronic supplementary information (ESI) available. See DOI: 10.1039/d1na00180a

area ratio from 11% to 58% and the SNR from 2.67 (flat surface) to 14.02 (grooved surface).

Here, we propose haircell structures on the porous PDMS surface for further SNR enhancement. We perform the theoretical analysis and experimental verification on the haircell structure design, achieving the higher SNR with the increased skin contact area compared to the previous studies.

Therefore, we demonstrate a porous PDMS pulsewave sensor with haircell structures, achieving a high WVTR of 486 $g^{-1} d^{-1}$
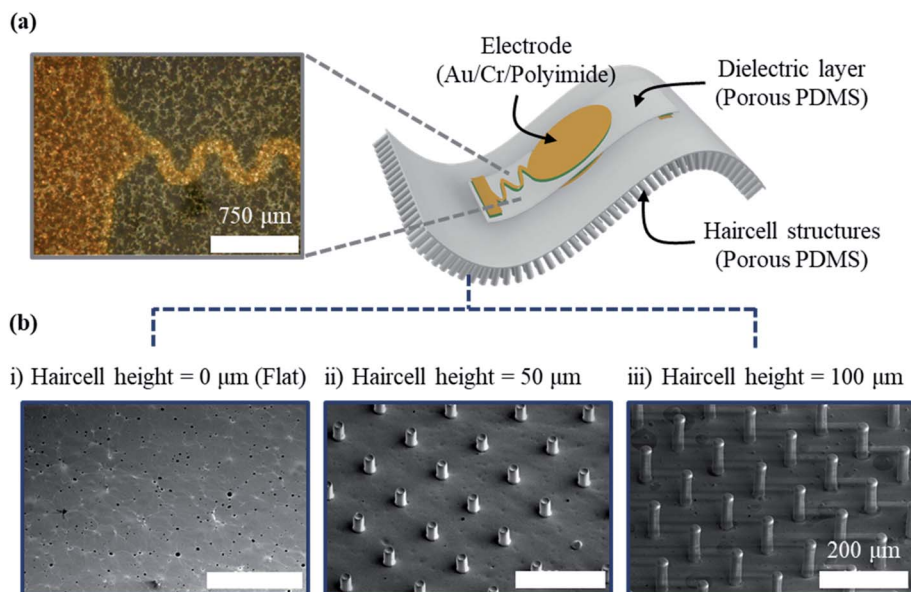

Fig. 1 Porous PDMS pulsewave sensors with haircell structures: (a) a magnified optical microscopy image of the electrode on the dielectric layer; (b) SEM images of the porous PDMS layers with the different haircell heights of (i) 0 μm (flat), (ii) 50 μm and (iii) 100 μm.
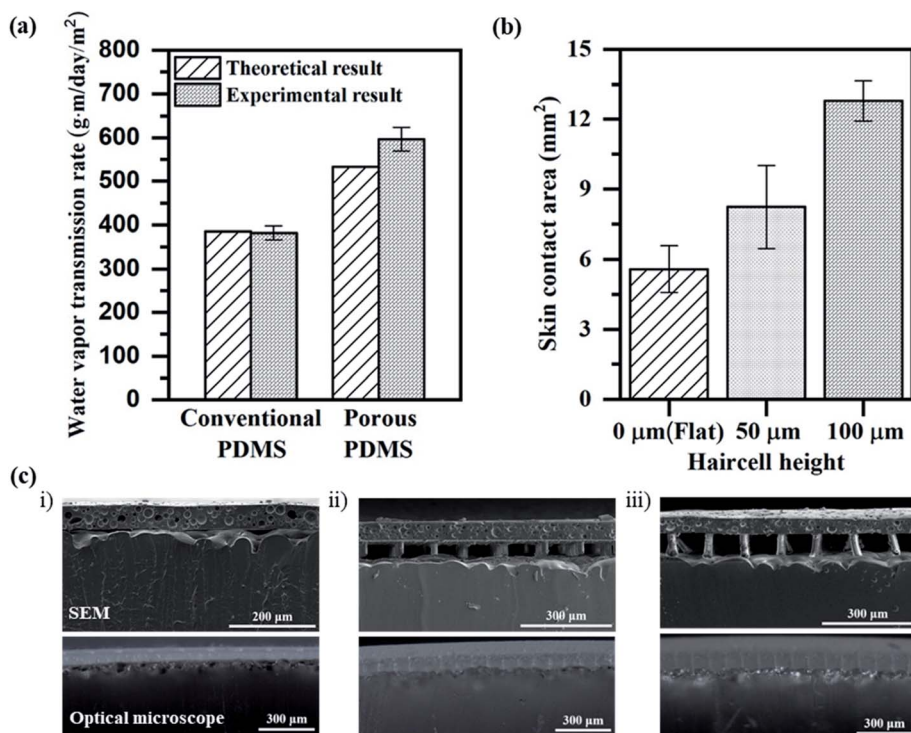

Fig. 2 The characteristics of the porous PDMS layers with the haircell structures: (a) the water vapor transmission rates, estimated and measured from the conventional PDMS layers and the porous PDMS layers having an identical thickness of 40 μm; (b) skin contact area of the porous PDMS layers without and with the haircell heights of 50 and 100 μm; (c) SEM and optical microscope images of the porous PDMS layers with the haircell heights of (i) 0 μm (flat), (ii) 50 μm and (iii) 100 μm, respectively contacted to the artificial skin.

m^{-2} with a high SNR of 22.89, for applications in skin-trouble free pulsewave monitoring in daily life.

Results and discussion

Fabrication of the porous PDMS pulsewave sensor with haircell structures

The porous PDMS pulsewave sensor with haircell structures (Fig. 1a) is composed of a capacitive pulsewave sensor layer for radial artery pulse measurement and haircell structures on the porous PDMS layer for increasing the skin contact area. The capacitive pulsewave sensor layer was fabricated by the evaporation of top and bottom gold/chromium (Au/Cr) electrodes on polyimide (PI) inter layers, spin-coated on a 70 μm-thick porous PDMS dielectric layer. The PI inter layers, having the high stiffness of 4.1 GPa, were used to prevent electrode crack. The porous PDMS layer with haircell structures were fabricated using a SU-8 photoresist as molds. The porous PDMS pulsewave

sensor with haircell structures was finally obtained by the assembly of the pulsewave sensor layer and the porous PDMS layer with haircell structures (see Method, Fig. S2 and S3†). Fig. 1b shows the three different prototypes of porous PDMS pulsewave sensors, respectively having the haircell heights of 0 (flat), 50, and 100 μm for conducting WVTR and SNR tests.

Finding a proper weight ratio of citric acid powders to PDMS, having uniform pore size and porosity, is crucial for WVTR enhancement. We compared a weight ratio that showed the minimum coefficient of variance (CV) value of the pore size and porosity among the porous PDMS layers with different weight ratios of 0.5 : 1, 1 : 1, 1.5 : 1, and 2 : 1. Among them, the weight ratio of 0.5 : 1 resulted in the minimum CV of the pore size and porosity, where the mean pore size and porosity were 21.08 μm and 45%, respectively (Table S1†). Hence, we determined the weight ratio of 0.5 : 1 for the porous PDMS layer. For better WVTR, the thinner porous PDMS layer is recommended. We decided the thickness of the porous PDMS layer to be as thin as
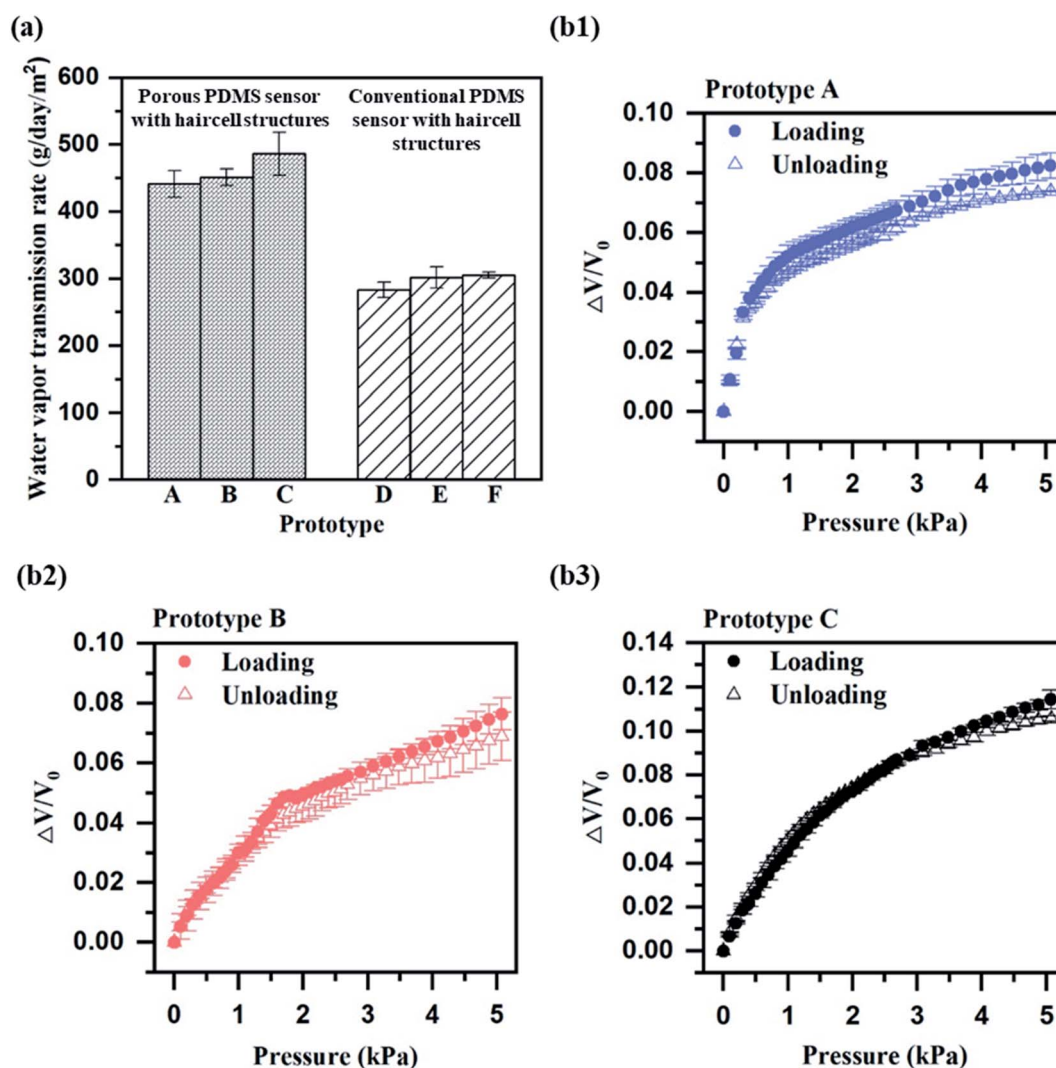

Fig. 3 Water vapor transmission rates and relative output voltage of the prototypes A–F, described in Results and discussion: (a) comparison of the water vapor transmission rates, measured from the prototypes A, B, C and the prototypes D, E, F (b1–b3). The relative output voltage, measured from the prototypes A, B, C by circuit during pressure loading and unloading cycles.

40 μm for successful detachment from the substrate. WVTR of the 40 μm-thick porous PDMS layer, thicker than the mean pore size of 21 μm, was measured to be 596.06 $g^{-1} d^{-1} m^{-2}$, which was greater than the human skin sweat rate (432 $g^{-1} d^{-1} m^{-2}$) as well as WVTR (382.45 $g^{-1} d^{-1} m^{-2}$) of the conventional PDMS layer. Fig. 2a shows that the experimental value of WVTR is well in agreement with the theoretical value of WVTR ($W_{\text{P-PDMS}}$), expressed as

$$W_{\text{P-PDMS}} = pW_{\text{pore}} + (1 - p)W_{\text{PDMS}} \qquad (1)$$

where p is the porosity of the porous PDMS layer, and W_{pore} and W_{PDMS} are the WVTR of the pore and 40 μm-thick conventional PDMS layer, respectively.

We conducted the skin attachment test (Table S2†) using the fabricated porous PDMS layer and the conventional PDMS layer to compare their skin trouble effect. Both layers were attached to the right forearm of one subject for 7 days. The conventional PDMS layer induced irritant contact dermatitis characterized by skin redness and itchiness. The porous PDMS layer showed no skin trouble, demonstrating its suitability for long-term and daily use.

We formed the haircell structures on the porous PDMS layer in order to increase the skin contact area effective to high SNR. The haircell diameter was determined as 30 μm, considering the average pore diameter of 21 μm. The haircell height should be greater than the average skin roughness[26] of 27 μm and smaller than the buckling height (h) of 120 μm at the radial artery pulse (P):

$$h = \sqrt{\frac{E \times \pi^3 \times r}{2^{10} \times 10^4 \times P}} \qquad (2)$$

where E and r are the elastic modulus and radius of the haircell, respectively. In order to decide the haircell height, we measured the contact area of three different haircell structures (height: 0 (flat), 50, 100 μm) with an artificial skin[27] (Fig. S4†). Out of

them, we chose the 100 μm-high haircell structures, resulting in the largest contact area (A) of 12.79 mm^2 (Fig. 2b):

$$A = A_{\text{total}}P_{\text{contracted haircells}} \qquad (3)$$

where A_{total} is the sum of individual haircell area and $P_{\text{contacted haircells}}$ is the ratio of the number of contacted haircells to the number of total haircells. We confirmed that the 100 μm-high haircell structures were in conformal contact (Fig. 2c) with the artificial skin. The inter-haircell gap of 100 μm-high haircell structures was determined to be 90 μm, which was at least equal to the lateral diffraction ($\delta = 90$ μm from eqn (4)) of buckled haircells for preventing the overlap between haircells.

$$\delta = e \left[\sec\left(\frac{\pi}{2} \sqrt{\frac{P}{P_{\text{cr}}}} \right) - 1 \right] \qquad (4)$$

where e is eccentricity (half of diameter, 15 μm), P is the radial artery pulse pressure, and P_{cr} is the critical buckling pressure (6 kPa).

The porous PDMS pulsewave sensor with haircell structures has the overall dimension of 2 cm × 2 cm × 210 μm, including the haircell structures having the diameter of 30 μm, the height of 100 μm, and the inter-haircell gap of 90 μm.

Water vapor transmission rate test

We verify the effect of the porous structures and haircell structures on WVTR improvement using an experimental set-up of Fig. S5.† In order to demonstrate the effect of the porous structures on WVTR enhancement, we prepared prototypes A, B, C, which were the porous PDMS pulsewave sensors having haircell heights of 0 (flat), 50, and 100 μm. Prototypes D, E, F, which were the PDMS pulsewave sensors having haircell heights of 0 (flat), 50, 100 μm, were also prepared to observe the haircell structure influence. WVTR of prototypes A, D and D, F was compared to determine the porous structures and haircell structures effect, respectively. Prototype A showed 56% higher
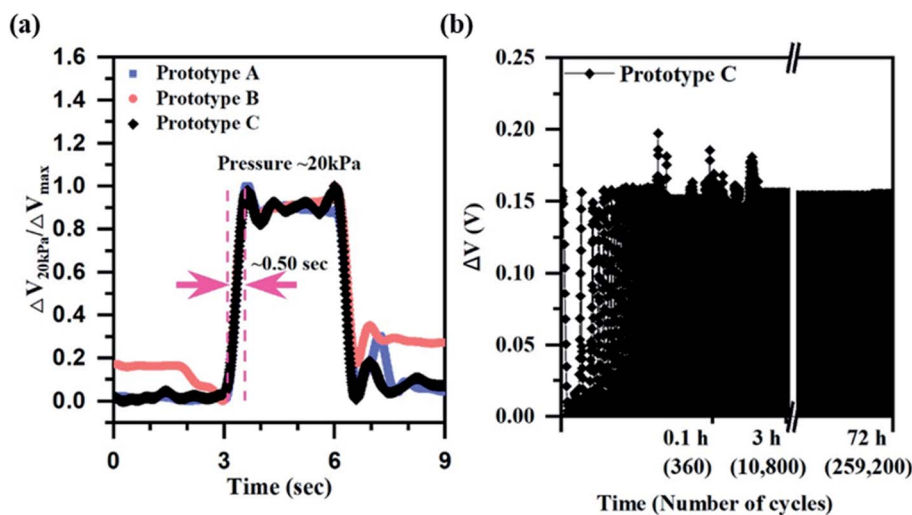

Fig. 4 Voltage response of prototypes A, B, C described in Results and discussion: (a) normalized output voltages of prototypes A, B and C at the pressure pulse of 20 kPa for 3 seconds; (b) output voltage change of prototype C under loading and unloading of 5 kPa at 1 Hz for 3 days, showing the stability of prototype C.

WVTR (440.84 g^{-1} d^{-1} m^{-2}) than prototype D (Fig. 3a), showing the effects of porous structures on WVTR. Prototype F indicated 8% higher WVTR (305.30 g^{-1} d^{-1} m^{-2}) than prototype D, demonstrating the influence of haircell structures on WVTR. We demonstrate that both porous structures and haircell structures influence WVTR enhancement, but the porous structures are the primary factor for enhanced WVTR. Furthermore, prototype C, including both porous structures and haircell structures, displayed the highest WVTR of 486.17 g^{-1} d^{-1} m^{-2} among other prototypes, and it is 13% higher than the human skin sweat rate.

Performance characterization

The sensor performance, including sensitivity, response time, linearity and hysteresis, was measured from prototypes A–C. All the sensor performances were measured by connecting to the circuit (Fig. S6†). The sensitivity of each prototype was measured in the narrow range of 0.02–0.04 kPa^{-1} (Fig. 3(b1–b3)). The response time of each prototype also showed a similar range of 0.43–0.50 s (Fig. 4a), but prototype C had the slowest response time of 0.50 s. The slow response time of prototype C is because of more elastic deformation on the haircell (eqn (5)) occurs as the haircell height increases, resulting in the longer elastic recovery time[28] (Fig. S7†).

$$\Delta L = \frac{L_0 P}{E} \tag{5}$$

where ΔL, L_0, and E are the deformation, initial height, and elastic modulus of the haircell, respectively, and P is the normal pressure applied to the haircell. Prototype C showed the highest linearity of 98% and the lowest hysteresis of 7.56%, respectively. Although prototype C has slow response time, it has high linearity and low hysteresis compared to the other prototypes. We
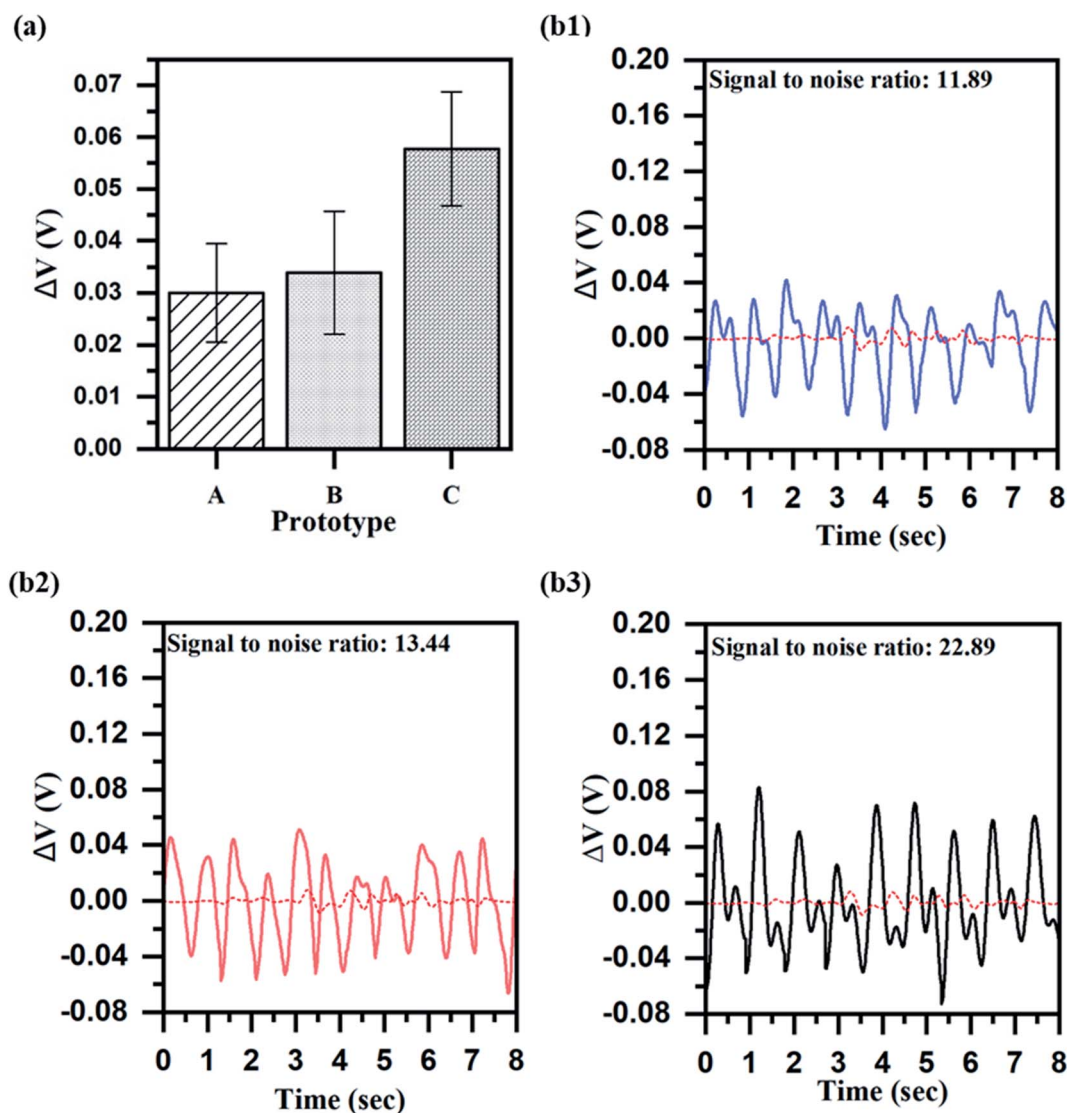

Fig. 5 Measurement of the radial artery pulsewave with prototypes A, B, C described in Results and discussion: (a) the output voltage changes of the prototypes at the radial artery pulse pressure of 5 kPa (b1–b3). The output voltage changes and signal-to-noise ratios of the prototypes A, B, C, where the dashed baselines indicate the noise levels without the radial artery pulse. The signal-to-noise ratio was defined as the average output voltage change for the pulse pressure over the standard deviation of the baseline.

found prototype C as the best design for measuring the radial artery pulse. In addition, we performed the stability test under 250 000 cycles loading and unloading at 5 kPa pressure for 3 days. Since prototype C showed stable output voltage change (Fig. 4b), it is confirmed that prototype C has good stability.

Human experiment for the measurement of the radial artery pulse

We applied prototypes A, B, and C to the human experiment for measuring the output voltage and SNR (eqn (6)) under the radial artery pulse (Fig. S8†).

$$\text{SNR} = \frac{\text{avg}(\Delta V_{\max})}{\sigma_{\text{baseline}}} \qquad (6)$$

where $\text{avg}(\Delta V_{\max})$ is the average of the output voltage change caused by the radial artery pulse and σ_{baseline} is the standard deviation of the baseline noise level without the radial artery pulse. Prototype C indicated the higher output voltage (Fig. 5a) of 0.058 V and SNR (Fig. 5(b1–b3)) of 22.89 than other prototypes. We found that the haircell structures were effective to SNR enhancement. In order to determine the effect of haircell structures on SNR improvement, we theoretically estimated the capacitance change (ΔC) of prototype A and C upon the radial artery pulse (P):

$$\Delta C = \varepsilon_0 \varepsilon_r \frac{A_{\text{elec}}}{\Delta t} \qquad (7)$$

$$\Delta t = \frac{P \times R \times t_0}{E \times A_{\text{elec}}} \qquad (8)$$

where ε_0 and ε_r are the absolute permittivity and the dielectric constant of porous PDMS, respectively, A_{elec} is the area of the electrode, t_1 and t_0 are the thickness of the porous PDMS dielectric layer with and without the radial artery pulse, respectively, and R is the ratio of the skin contact area to the bottom surface area of the prototype. The capacitance change increased when the pulse pressure was well transferred to the dielectric layer of the prototypes, and the transferred pulse pressure was proportional to the skin contact area of the prototypes. The results of the previous contact area test were used in theoretical estimation. Prototype C had 129% larger contact area than that of prototype A, resulting in improved pulse pressure transfer to the dielectric layer compared to prototype A. Prototype C presented 100% higher capacitance change than prototype A, which was well in agreement with the ratio of the SNR increase (93%). Therefore, we verify that prototype C having the haircell structures can improve the SNR by increasing the contact area with the skin, compared to prototype A having no haircell structures.

Conclusions

This study presents a porous PDMS pulsewave sensor with haircell structures for high WVTR and high SNR. In order to improve WVTR, we developed a noble porous PDMS layer in thin thickness (40 μm) and high porosity (45%) by the crystallization and dissolution of citric acid powders in PDMS. On the

noble porous PDMS layer, we formed haircell structures with the diameter of 30 μm, height of 100 μm and inter-haircell gap of 90 μm to increase effective skin contact area, thus enhancing SNR. The present pulsewave sensor shows the improved WVTR of 486.17 $\text{g}^{-1}\,\text{d}^{-1}\,\text{m}^{-2}$ and the SNR of 22.89, which are 72% and 757% greater than those of conventional PDMS pulsewave sensors without haircell structures, respectively. Moreover, the improved WVTR is 13% higher than the human skin sweat rate (432 $\text{g}^{-1}\,\text{d}^{-1}\,\text{m}^{-2}$). The present pulsewave sensor is suitable for long-term pulsewave monitoring in daily-life without skin trouble.

Method

Fabrication of the haircell structure mold

A SU-8 negative photoresist (SU-8 2050, Micro Chem) was used as the haircell structure mold. A 100 μm-thick SU-8 2050 was spin-coated on the silicon wafer (Si wafer) and soft baked at 65/95 °C for 5/30 min. The soft baked SU-8 was exposed by UV energy with 64 mJ cm^{-2} and post baked at 65/95 °C for 5/10 min. The post baked SU-8 was sonicated in a SU-8 developer (Micro Chem) for 5 min to obtain the haircell structure mold.

Fabrication of the PDMS with crystalized citric acid powders

Polydimethyl siloxane (PDMS, Sylgard 184, Dow Corning) was stirred with toluene (Signa Aldrich), citric acid monohydrate (Sigma Aldrich), and ethanol (99.9% absolute, Oci) at 100 rpm and room temperature for 30 min on hotplate (Wisestir, Wised). Toluene and ethanol were evaporated from the mixture while stirring at 100 rpm and 150 °C for 3 h 52 min in order to crystallize the citric acid powders in PDMS. The detailed fabrication method is indicated in our previous research.[29]

Fabrication of the porous PDMS layer with haircell structures

The porous PDMS layer with haircell structures was fabricated by a well-known polymer molding technique. In order to facile demold the porous PDMS layer with haircell structures from the mold, trichloro(1H,1H,2H,2H-perfluorooctyl)silane (Sigma Aldrich) was vaporized on the mold under vacuum condition for 50 min. Subsequently, the PDMS with crystallized citric acid powders and a curing agent were mixed in a weight ratio of 15 : 1 and spin-coated on the silane treated mold for the thickness of 40 μm, followed by solidification at 100 °C for 1 h. The citric acid powder in PDMS was dissolved in ethanol for 1 min 30 s to form the porous PDMS layer with haircell structures on the mold.

Fabrication of the pulsewave sensor layer

The pulsewave sensor was composed of a bottom electrode, a porous PDMS dielectric layer, and a top electrode. 100/10 nm-thick Au/Cr was evaporated and patterned on the silane-treated Si wafer for the bottom electrode. Subsequently, a 1.5 μm-thick polyimide (PI) layer was spin-coated and patterned on the bottom electrode. In order to increase the adhesion of the PI layer surface, the PI layer was treated with (3-mercaptopropyl)trimethoxysilane (MPTMS, Sigma Aldrich) and (3-glycidyloxy-

propyl) trimethoxysilane (GPTMS, Sigma Aldrich). The mixture of PDMS with crystallized citric acid powders and curing agent (weight ratio: 15 : 1) was spin-coated on the silane-treated PI layer for the thickness of 70 μm and cured at 100 °C for 1 h. The citric acid powders were dissolved in ethanol to obtain the porous PDMS dielectric layer on the PI layer. Then, a 1.5 μm-thick PI layer was spin-coated and patterned on an oxidized Si wafer for the top electrode. On the PI layer, 10/100 nm-thick Cr/Au was evaporated and patterned. The top electrode with the PI layer was released from the substrate using a polyvinyl alcohol tape (PVA tape, Water soluble wave solder tape 5414, 3M). Released top electrode with the PI layer was aligned and assembled with the porous PDMS dielectric layer with the bottom electrode using a custom-made zig to obtain the pulsewave sensor layer. We finally aligned and assembled the pulsewave sensor layer to the porous PDMS layer with haircell structures in order to complete the porous PDMS pulsewave sensor with haircell structures.

Human experiment

The human experiment was approved by KAIST Institutional Review Board (IRB). All the experiment performed on human subjects were carried out with informed consent under the guidelines and regulations of the KAIST IRB, ID number KH2011-18.

Author contributions

M. Seok, S. Yoon, and Y.-H. Cho conceived this research. M. Seok designed and simulated the sensors. M. Seok and M. Kim fabricated the sensors. M. Seok and Y.-H. Cho analysed the material properties and the electrical signals of the sensors and wrote the paper. All authors reviewed the manuscript and provided feedback.

Conflicts of interest

There are no conflicts to declare.

Acknowledgements

References

1 D. M. Drotlef, M. Amjadi, M. Yunusa and M. Sitti, Bioinspired Composite Microfibers for Skin Adhesion and Signal Amplification of Wearable Sensors, *Adv. Mater.*, 2017, 1701353.

2 D.-H. Kim, N. Lu, R. Ma, Y.-S. Kim, R.-H. Kim, S. Wang, J. Wu, S. M. Won, H. Tao, A. Islam, K. J. Yu, T.-i. Kim, R. Chowdhury, M. Ying, L. Xu, M. Li, H.-J. Chung, H. Keum, M. McCormick and J. A. Rogers, Epidermal Electronics, *Science*, 2011, **333**(6044), 838–843.

3 S. Yoon, J. K. Sim and Y. H. Cho, A Flexible Piezoelectric Pulsewave Energy Harvester for Application to High-Efficiency Multi-Functional Skin Patches, *J. Microelectromech. Syst.*, 2016, **25**(2), 388–393.

4 J. Park, M. Kim, Y. Lee, H. S. Lee and H. Ko, Fingertip skin-inspired microstructured ferroelectric skins discriminate static/dynamic pressure and temperature stimuli, *Sci. Adv.*, 2015, **1**(9), e1500661.

5 J. Kim, N. Kim, M. Kwon and J. Lee, Attachable Pulse Sensors Integrated with Inorganic Optoelectronic Devices for Monitoring Heart Rates at Various Body Locations, *ACS Appl. Mater. Interfaces*, 2017, **9**(31), 25700–25705.

6 S. Gong, W. Schwalb, Y. Wang, Y. Chen, Y. Tang, J. Si, B. Shirinzadeh and W. Cheng, A wearable and highly sensitive pressure sensor with ultrathin gold nanowires, *Nat. Commun.*, 2014, **5**, 1–8.

7 H. Park, Y. R. Jeong, J. Yun, S. Y. Hong, S. Jin, S. J. Lee, G. Zi and J. S. Ha, Stretchable Array of Highly Sensitive Pressure Sensors Consisting of Polyaniline Nanofibers and Au-Coated Polydimethylsiloxane Micropillars, *ACS Nano*, 2015, **9**(10), 9974–9985.

8 J. Kim, D. G. Seo and Y. H. Cho, A flexible skin piloerection monitoring sensor, *Appl. Phys. Lett.*, 2014, **104**(25), 253502.

9 Y. Liu, J. J. S. Norton, R. Qazi, Z. Zou, K. R. Ammann, H. Liu, L. Yan, P. L. Tran, K. I. Jang, J. W. Lee, D. Zhang, K. A. Kilian, S. H. Jung, T. Bretl, J. Xiao, M. J. Slepian, Y. Huang, J. W. Jeong and J. A. Rogers, Epidermal mechano-acoustic sensing electronics for cardiovascular diagnostics and human-machine interfaces, *Sci. Adv.*, 2016, **2**(11), e1601185.

10 Q. J. Sun, J. Zhuang, S. Venkatesh, Y. Zhou, S. T. Han, W. Wu, K. W. Kong, W. J. Li, X. Chen, R. K. Y. Li and V. A. L. Roy, Highly Sensitive and Ultrastable Skin Sensors for Biopressure and Bioforce Measurements Based on Hierarchical Microstructures, *ACS Appl. Mater. Interfaces*, 2018, **10**(4), 4086–4094.

11 C. M. Boutry, A. Nguyen, Q. O. Lawal, A. Chortos, S. Rondeau-Gagné and Z. Bao, A Sensitive and Biodegradable Pressure Sensor Array for Cardiovascular Monitoring, *Adv. Mater.*, 2015, **27**(43), 6954–6961.

12 C. Luo, J. Jia, Y. Gong, Z. Wang, Q. Fu and C. Pan, Highly Sensitive, Durable, and Multifunctional Sensor Inspired by a Spider, *ACS Appl. Mater. Interfaces*, 2017, **9**(23), 19955–19962.

13 Y. Song, H. Chen, Z. Su, X. Chen, L. Miao, J. Zhang, X. Cheng and H. Zhang, Highly Compressible Integrated Supercapacitor–Piezoresistance-Sensor System with CNT–PDMS Sponge for Health Monitoring, *Small*, 2017, **13**(39), 1702091.

14 L.-Q. Tao, K.-N. Zhang, H. Tian, Y. Liu, D.-Y. Wang, Y.-Q. Chen, Y. Yang and T.-L. Ren, Graphene-Paper Pressure Sensor for Detecting Human Motions, *ACS Nano*, 2017, **11**(9), 8790–8795.

15 S. Yoon, J. K. Sim and Y.-H. Cho, A Flexible and Wearable Human Stress Monitoring Patch, *Sci. Rep.*, 2016, **6**, 23468.

16 K. He, Y. Hou, C. Yi, N. Li, F. Sui, B. Yang, G. Gu, W. Li, Z. Wang, Y. Li, G. Tao, L. Wei, C. Yang and M. Chen, *Nano Energy*, 2020, **73**, 104743.

17 M. Chen, J. Xia, J. Zhou, Q. Zeng, K. Li, K. Fujisawa, W. Fu, T. Zhang, J. Zhang, Z. Wang, Z. Wang, X. Jia, M. Terrones, Z. X. Shen, Z. Liu and L. Wei, *ACS Nano*, 2017, **11**, 9191–9199.

18 M. Chen, Z. Wang, X. Ge, Z. Wang, K. Fujisawa, J. Xia, Q. Zeng, K. Li, T. Zhang, Q. Zhang, M. Chen, N. Zhang, T. Wu, S. Ma, G. Gu, Z. Shen, L. Liu, Z. Liu, M. Terrones and L. Wei, *Matter*, 2020, **2**, 666–679.

19 M. Chen, K. Li, G. Cheng, K. He, W. Li, D. Zhang, W. Li, Y. Feng, L. Wei, W. Li, G. Zhong and C. Yang, *ACS Appl. Mater. Interfaces*, 2019, **11**, 2551–2558.

20 N. A. S. Taylor and C. A. Machado-Moreira, Regional variations in transepidermal water loss, eccrine sweat gland density, sweat secretion rates and electrolyte composition in resting and exercising humans, *Extreme Physiol. Med.*, 2013, **2**(1), 1–30.

21 A. Miyamoto, S. Lee, N. F. Cooray, S. Lee, M. Mori, N. Matsuhisa, H. Jin, L. Yoda, T. Yokota, A. Itoh, M. Sekino, H. Kawasaki, T. Ebihara, M. Amagai and T. Someya, Inflammation-free, gas-permeable, lightweight, stretchable on-skin electronics with nanomeshes, *Nat. Nanotechnol.*, 2017, 1–7.

22 M. Ha, S. Lim, S. Cho, Y. Lee, S. Na, C. Baig and H. Ko, Skin-Inspired Hierarchical Polymer Architectures with Gradient Stiffness for Spacer-Free, Ultrathin, and Highly Sensitive Triboelectric Sensors, *ACS Nano*, 2018, **12**(4), 3964–3974.

23 S. Kang, J. Lee, S. Lee, S. G. Kim, J. K. Kim, H. Algadi, S. Al-Sayari, D. E. Kim, D. E. Kim and T. Lee, Highly Sensitive Pressure Sensor Based on Bioinspired Porous Structure for Real-Time Tactile Sensing, *Adv. Electron. Mater.*, 2016, **2**(12), 1600356.

24 C. Yu, C. Yu, L. Cui, Z. Song, X. Zhao, Y. Ma and L. Jiang, Facile Preparation of the Porous PDMS Oil-Absorbent for Oil/Water Separation, *Adv. Mater. Interfaces*, 2017, **4**(3), 1600862.

25 Y. Park, J. Shim, S. Jeong, G. R. Yi, H. Chae, J. W. Bae, S. O. Kim and C. Pang, Microtopography-Guided Conductive Patterns of Liquid-Driven Graphene Nanoplatelet Networks for Stretchable and Skin-Conformal Sensor Array, *Adv. Mater.*, 2017, **29**(21), 1606453.

26 M. Darvin, A. Patzelt, S. Gehse, S. Schanzer, C. Benderoth, W. Sterry and J. Lademann, Cutaneous concentration of lycopene correlates significantly with the roughness of the skin, *Eur. J. Pharm. Biopharm.*, 2008, **69**(3), 943–947.

27 Y. Pang, K. Zhang, Z. Yang, S. Jiang, Z.-Y. Ju, Y. Li, X. Wang, D.-Y. Wang, M. Jian, Y. Zhang, R. Liang, H. Tian, Y. Yang and T.-L. Ren, Epidermis Microstructure Inspired Graphene Pressure Sensor with Random Distributed Spinosum for High Sensitivity and Large Linearity, *ACS Nano*, 2018, **12**(3), 2346–2354.

28 S. M. Kim, C. Pang, D. Kang, T. Kim, W. G. Bae and K.-Y. Suh, Bioinspired Reversible Interlocker Using Regularly Arrayed High Aspect-Ratio Polymer Fibers, *Adv. Mater.*, 2011, **24**(4), 475–479.

29 S. Yoon, M. Seok, M. Kim and Y. H. Cho, Wearable porous PDMS layer of high moisture permeability for skin trouble reduction, *Sci. Rep.*, 2021, **11**(1), 1–11.